Chapter 4

Effect of Acidity on Secondary Organic Aerosol Formation from Isoprene*

---

*This chapter is reproduced by permission from “Effect of Acidity on Secondary Organic Aerosol Formation from Isoprene” by Jason D. Surratt, Michael Lewandowski, John H. Offenberg, Mohammed Jaoui, Tadeusz E. Kleindienst, Edward O. Edney, and John H. Seinfeld, *Environmental Science & Technology*, 41 (15), 5363–5369, 2007. Copyright 2007 by the American Chemical Society.

4.1 Abstract

The effect of particle-phase acidity on secondary organic aerosol (SOA) formation from isoprene is investigated in a laboratory chamber study, in which the acidity of the inorganic seed aerosol was controlled systematically. The observed enhancement in SOA mass concentration is closely correlated with increasing aerosol acidity ($R^2 = 0.979$). Direct chemical evidence for acid-catalyzed particle-phase reactions was obtained from the SOA chemical analyses. Aerosol mass concentrations for the 2-methyltetrols, as well as the newly identified sulfate esters, both of which serve as tracers for isoprene SOA in ambient aerosols, increased significantly with enhanced aerosol acidity. Aerosol acidities, as measured in nmol H^+ m^{-3}, employed in the present study are in the same range as those observed in tropospheric aerosol collected from the eastern U.S.

4.2 Introduction

Increased acidity of inorganic seed aerosol in laboratory experiments has been shown to lead to enhanced secondary organic aerosol (SOA) formation from the oxidation of several volatile organic compounds (VOCs) (*1−7*). Acid-catalyzed particle-phase reactions leading to the formation of high-molecular-weight (MW) species, some of which are oligomeric in nature, have been proposed to explain these observed enhancements. Such reactions include the reactive uptake of volatile aldehydes or ketones via peroxyhemiacetal formation (*8*, *9*), hydration, hemiacetal/acetal formation, and/or aldol condensation (*1*). Acidity derived from inorganic seed aerosol is not necessarily a prerequisite for the generation of high-MW products (*4*, *5*, *10*, *11*); particle-phase acidity derived from photochemically generated organic acids appears to be sufficient. Currently, the role of particle-phase reactions in ambient $PM_{2.5}$ is unclear, as supportive chemical composition data are lacking and many proposed reactions are not thermodynamically favorable under ambient conditions (*12*, *13*). Particle-phase sulfate esterification products have been shown to be present in both laboratory-generated and ambient aerosol (*14-17*); however, quantification of these products is still needed in order to establish their overall importance to ambient $PM_{2.5}$.

Recent work has shown that SOA formation from isoprene (2-methyl-1,3-butadiene, C_5H_8) is significant (*6*, *7*, *11*, *14, 18−23*). Despite lower SOA yields than those of other biogenic VOCs (*6*, *20*, *21*, *23*), including SOA formation from isoprene in global model simulations leads to significant increases in predicted SOA and may help explain deviations between observed and predicted SOA (*22*). It is now understood that the level of NO_x plays a crucial role in SOA formation from isoprene (as well as other

VOCs) (*11*, *20*, 2*1*). In addition, decreases in relative humidity (RH) have been found to lead to a decrease in the volatility of isoprene SOA (*23*); however, as suggested by these authors, further investigation is warranted owing to inconsistencies in the measured SOA yields. Despite previous observations of enhancement of SOA from isoprene under acidic conditions (*6*, *7*, *11*, *14*), many of which were measured at only one level of enhanced acidity, the effect of particle-phase acidity on SOA formation from isoprene remains a key unresolved issue.

In the present work, the effect of particle-phase acidity, as measured by the hydrogen ion air concentration (denoted as $[H^+]_{air}$; expressed in nmol m^{-3}), on SOA formation from isoprene in the presence of NO is investigated in a four-stage, steady-state laboratory chamber study. The acidity of the inorganic seed aerosol was controlled by systematically increasing the acidity of the atomizing solution. All other experimental parameters were held constant. At each stage of the experiment, complete steady-state gas- and particle-phase measurements were conducted, as well as chemical composition analysis of the resultant SOA. We show that the measured organic carbon (OC) mass concentration (mgC m^{-3}) is directly correlated to the measured aerosol acidity. In addition, several of the known isoprene SOA tracer compounds increase with increasing aerosol acidity, suggesting the presence of acid-catalyzed particle-phase reactions, and thus providing insights into the chemical mechanism for SOA formation from isoprene.

4.3 Experimental Section

4.3.1 Chamber Procedures

To investigate the role of particle-phase acidity on SOA formation from isoprene, a four-stage photooxidation experiment was conducted in a 14.5 m^3 Teflon-coated stainless steel indoor chamber, operated in a dynamic mode (i.e. as a continuous stirred tank reactor). Details of the chamber and its operation are described elsewhere (*6*). Isoprene and NO were continuously injected from high-pressure cylinders into the reaction chamber through a mixing manifold. Isoprene and NO concentrations were constant throughout the experiment, as well as other experimental parameters such as temperature (29 °C) and relative humidity (30 %). The latter were measured with an Omega digital thermo-hydrometer (model RH411, Omega Engineering, Inc., Stamford, CT). The flow rate through the chamber was such that the chamber residence time was 4 h.

The only experimental parameter to change throughout each stage of this experiment was the acidity of the inorganic seed aerosol. In Stage 1, the inorganic seed aerosol was generated by atomization from an aqueous solution containing 0.5 mg L^{-1} of ammonium sulfate. Teflon filter (PALL Life Sciences, 47-mm diameter, 0.45-mm pore size, Teflo Membrane) samples for $[H^+]_{air}$ determination and glass fiber filters (Pall Gelman Laboratory, 47-mm diameter, Teflon-impregnated, Ann Arbor, MI) for organic analysis were collected during this stage. In Stage 2, the inorganic seed aerosol was generated by atomization from an aqueous solution containing both 41 mg L^{-1} ammonium sulfate and 60 mg L^{-1} sulfuric acid. Both Teflon and glass fiber filters were collected during this stage as well. An additional Teflon filter (PALL Life Sciences, 47-mm diameter, 2.0-mm pore size, Zefluor membrane) was collected at this stage for $[H^+]_{air}$ determination. In Stage 3, the inorganic seed aerosol was generated by atomizing an aqueous solution containing 90 mg L^{-1} sulfuric acid. Only Teflon filters (Teflo Membrane type only) for $[H^+]_{air}$ determination were collected during this stage. In the final stage, Stage 4, a 90 mg L^{-1} sulfuric acid solution was used for the generation of the inorganic seed aerosol, but during this stage, glass fiber filters for organic analysis were taken in addition to the Teflon (Teflo and Zefluor Membrane types) filters used for $[H^+]_{air}$ measurements. For each of these stages, steady-state gas- and particle-phase measurements were conducted after 3 residence times following the change in the acidity of the atomizing solution. Gas-phase carbonyl products were measured by a 2,4-dinitrophenyl-hydrazine technique previously described (*6*). In order to collect sufficient aerosol mass for the offline chemical analysis techniques, glass fiber and Teflon filters were collected for 24 h and 4 h, respectively. During filter sampling, glass fiber filters and Teflon filters, with a Zefluor Membrane, were preceded by a carbon-strip organic denuder. The Teflon filters with a Teflo Membrane were collected undenuded.

Semi-continuous measurements of the isoprene, NO, NO_x, O_3, and organic carbon (OC) concentrations were carried out throughout all of the stages of the experiment. Inlet manifold and chamber concentrations of isoprene were measured using a cryogenic trap for sample collection with analysis by gas chromatography (GC) with flame ionization detection (Hewlett Packard, Model 5890 GC, Palo Alto, CA). NO and NO_x concentrations were measured with a TECO model 42C oxides of nitrogen chemiluminescent analyzer. O_3 was measured with a Bendix ozone monitor (model 8002, Lewisburg, WV). OC mass concentrations (mgC m^{-3}) were measured using an automated, semi-continuous elemental carbon (EC)-OC instrument developed by Sunset Laboratories, described in detail elsewhere (*7*). Briefly, the duty cycle for this measurement was 0.75 h (i.e. 0.5 h and 0.25 h sampling and analysis time, respectively), and the analysis was conducted using the thermal-optical technique as described by Birch and Cary (*24*).

4.3.2 Glass Fiber Filter Extraction and Organic Analysis

Glass fiber filters were collected for SOA composition analysis. Three were collected for each stage of the experiment in order to have sufficient sample available for the following suite of analytical techniques: gas chromatography/mass spectrometry (GC/MS), liquid chromatography/electrospray ionization-quadrupole mass spectrometry (LC/ESI-MS), ESI-ion trap mass spectrometry (ESI-ITMS), and matrix-assisted laser desorption ionization-time-of-flight mass spectrometry (MALDI-TOFMS). It should be noted that the ESI-ITMS results are not presented, as they were shown in our previous study that chemically characterized organosulfates found in isoprene and a-pinene SOA (*14*). Glass fiber filters used for GC/MS analysis were extracted by sonication for 1 h in a GC^2-grade methanol/GC^2-grade dichloromethane solvent mixture (50:50) to which 20 mg of *cis*-ketopinic acid was added as an internal standard. The resultant extracts were dried and derivatized by a *bis*(trimethylsilyl) trifluoroacedimide (BSTFA) containing 1% trimethylchlorosilane (TMCS) procedure, described in detail elsewhere (*25*). GC/MS analysis was conducted on a ThermoQuest (Austin, TX) GC coupled to an ion-trap MS operated in the chemical ionization (CI) mode (*26*). Glass fiber filters used for ESI and MALDI techniques were extracted by sonication for 40 min in HPLC-grade methanol (*11*). The solvent composition of the resultant sample extract was the same as that for ESI and MALDI analysis. Details of the operating conditions used for the LC/ESI-MS, ESI-ITMS, and MALDI-TOFMS instruments are described elsewhere (*11*).

4.3.3 Teflon Filter Extractions and $[H^+]_{air}$ Determination

Collected Teflon (Teflo and Zeflour Membranes) filters were used for determining the hydrogen ion concentration in the aerosol per unit volume of air, expressed in nmol m^{-3}. Henceforth, we denote this quantity as $[H^+]_{air}$. In the absence of any available techniques for directly measuring the pH of aqueous atmospheric aerosols, $[H^+]_{air}$ is measured as follows. A volume of air (vol-air), measured in m^3, containing aerosol, is collected onto a Teflon filter. The filter is then extracted in a volume of deionized water (vol-H_2O), measured in mL. In the present study, the filters were extracted by sonication for 30 min in 10 mL of deionized water. After samples cooled to room temperature, the pH of the water extract was then immediately measured with a Mettler-Toledo MP220 pH meter using an InLab 413 pH electrode. The resulting aqueous hydrogen ion concentration ($[H^+]_{aq\text{-}extract}$) is expressed in moles per mL of deionized water. The total number of moles of hydrogen ion collected on the filter is then the product of $[H^+]_{aq\text{-}extract}$ and vol-H_2O. The average air concentration of hydrogen ion in the air sample collected, i.e. the number of moles of hydrogen ion per m^3 of air, is expressed as $[H^+]_{air} = ([H^+]_{aq\text{-}extract} * \text{vol-}H_2O)/\text{vol-air}$. $[H^+]_{air}$ in nmol m^{-3} is then obtained by multiplying by 1×10^9, which is comparable to prior field measurements (*27–29*).

4.4 Results

Table 4.1 summarizes the input conditions used in the present study. As stated previously, the only input parameter changed during each stage of the experiment was the acidity of the inorganic seed aerosol. The input isoprene concentration remained stable throughout the experiment. A relatively high isoprene to NO ratio was used to ensure substantial SOA formation (*20*, *21*).

The steady-state gas-phase concentrations for all stages of the experiment are summarized in Table 4.2. Steady-state gas-phase concentrations of isoprene, NO, and NO_x remained fairly constant throughout the experiment. Formaldehyde was the most abundant gas-phase carbonyl oxidation product detected in all stages of the experiment, followed by methacrolein and methyl vinyl ketone, respectively, consistent with previous studies involving photooxidation of isoprene (*6*, *30*, *31*). Despite the glyoxal (and to some extent acrolein) mixing ratios slightly increasing with the acidity of the inorganic seed aerosol, no obvious trends were observed for the other measured gas-phase carbonyl oxidation products. The measured O_3 was observed to decrease slightly with increasing acidity of the inorganic seed aerosol, whereas the measured HNO_3 increased slightly.

Reacted isoprene and steady-state particle-phase concentrations for all stages of the experiment are summarized in Table 4.3. The reacted isoprene concentration was relatively constant throughout all stages. The OC mass as well as the measured $[H^+]_{air}$ increased with each stage of the experiment. As shown in Figure 4.1, the measured OC is linearly correlated with the measured $[H^+]_{air}$ (R^2 = 0.979). The two extra data points in Figure 4.1, which are not listed in Table 4.3, arise from the analysis of the two collected Zelfuor Membrane type of Teflon filters from Stage 2 ($[H^+]_{air}$ = 253 nmol m^{-3}) and Stage 4 ($[H^+]_{air}$ = 529 nmol m^{-3}). The consistency of the duplicate $[H^+]_{air}$ measurements shown in Figure 4.1 for Stages 2 and 4, which were conducted from two different types of Teflon filters (one collected with a denuder and one without), suggests that artifacts were not introduced during sample collection and analysis.

SOA composition data are consistent with the particle-phase measurements discussed above. Figure 4.2 shows GC/MS extracted ion chromatograms (EICs) (*m/z*

165, 321, 409) for Stages 1, 2, and 4, respectively. Compounds identified in these EICs correspond to the known indicator compounds for SOA formation from isoprene (*6*, *19*), which include 2-methylglyceric acid and the 2-methyltetrols (2-methylthreitol and 2-methylerythritol). The ions selected for the EICs correspond to the $[MH + CH_4]^+$ ions of the trimethylsilylated derivatives of 2-methylglyceric acid (*m/z* 321) and the 2-methyltetrols (*m/z* 409) and to the $[M - OSi(CH_3)_3]^+$ ion of the trimethylsilylated *cis*-ketopinic acid (*m/z* 165). Comparison of these three EICs shows that the 2-methyltetrol peak areas increase in absolute abundance from Stages 1, 2, and 4, respectively, indicating that 2-methyltetrol formation is dependent upon the aerosol acidity. 2-Methyltetrol formation was found to be similarly enhanced in the prior study of Edney et al. (*6*); in that study, only one level of acidity was investigated, which was generated by SO_2 photooxidation. In contrast to the 2-methyltetrols, the peak areas associated with 2-methylglyceric acid remain relatively constant throughout the experiment, which suggests that aerosol acidity does not play a role in its formation. Surratt et al. (*11*) recently showed that the level of NO_x could be a key factor in the formation of 2-methylglyceric acid and its corresponding oligomers.

Figure 4.3 shows the GC/MS EICs (*m/z* 407, 495, and 597) for Stages 1, 2, and 4, respectively, of selected high-mass products. The ions selected for the EICs correspond to the $[M - CH_3]^+$ ions of the trimethylsilylated derivatives. The most abundant chromatographic peaks in each stage are associated with the compounds with the derivatized MW of 510, previously characterized as 2-methylglyceric acid dimers (*11*, *32*) and produced from the particle-phase esterification of two 2-methylglyceric acid monomers. As for the 2-methyltetrols, the formation of these species is enhanced by aerosol acidity; however, there is not an obvious difference in the amounts between the two most acidic stages. The multiple chromatographic peaks associated with the derivatized MW of 510 are most likely a result of different structural isomers (e.g. linear and branched), consistent with previous work (*11*, *32*). The chromatographic peaks associated with the compounds of derivatized MW 422 are present only when acidic inorganic seed aerosol is present, and increase in abundance with enhanced aerosol acidity. The derivatized MW 612 products are observed only at the acidic conditions (Stages 2 and 4) and little differences are observed between their peak areas. The derivatized MW 422 and 612 SOA products are currently unidentified. It should be noted that no evidence was found in our (−)ESI-MS and GC/MS data for oligoesters larger than the dimer form, indicating that the extent of particle-phase esterification was not as large as previously observed (*11*). This could be a result of the higher RH and/or the lower NO_x conditions employed in the current study.

In addition to the GC/MS elucidated SOA products, a wide array of sulfate esters were identified in this study by (−)ESI-MS methods; the chemical structures of these SOA components have been characterized recently by Surratt et al. (*14*). Sulfate esters were observed in Stages 2 and 4, whereas no sulfate esters were observed in Stage 1. Stage 4 SOA exhibited the widest array of sulfate esters. Sulfate esters of MW 216 and 261 were found to produce two of the largest chromatographic peaks detected by the (−)LC/ESI-MS technique for Stages 2 and 4. Owing to their detection in both laboratory-generated and ambient aerosol, and unambiguously forming from isoprene-specific oxidation products, these two sulfate esters (MW 216 and 261) were suggested as indicator compounds for SOA formation from isoprene under acidic conditions (*14*). The chromatographic peak area for the sulfate ester of MW 261 increased significantly when comparing Stage 4 to Stage 2, whereas the chromatographic peak areas remained fairly constant for the sulfate ester of MW 216.

Estimated aerosol mass concentrations (ng m^{-3}) for the GC/MS and (−)LC/ESI-MS detected SOA products are summarized and shown in Figure 4.4. SOA products detected by GC/MS and (−)LC/ESI-MS were quantified using surrogate standard calibration curves generated from *cis*-ketopinic acid and sodium propyl sulfate, respectively. Propyl sulfate was found to have a retention time that is within +/- 1.5 min of all quantified sulfate esters. Until authentic standards become available for these sulfate esters, quantification must be conducted in this manner.

In addition to these products, (+)MALDI-TOFMS spectra using a graphite matrix were collected for Stages 1, 2, and 4, respectively, and are shown in Figure 4.5 to demonstrate the effect of particle-phase acidity on the formation of high-MW products (≥ 200 Da). These spectra are directly comparable owing to the same amount of sample extract analyzed, as well as the same amount of chamber air sampled for each stage of the experiment. Common 14, 16, 18 Da differences observed in each stage are indicative of oligomeric SOA, which is consistent with prior work (*11*, *23*, *33*). Even though MALDI-MS is not a quantitative method, from the spectra shown in Figure 4.5, one is able to conclude that the relative amounts (intensities) of the oligomeric high-MW products increase with increasing aerosol acidity. In addition, the MWs of these high-mass SOA products increase up to approximately 800 Da with increasing aerosol acidity, as found in the mass spectrum for Stage 4. Although the MALDI data do not yield any further information, it was found that the MWs of the previously characterized isoprene sulfate esters (*14*) have a corresponding $[M + Na]^+$ ion in Figure 4.5 for Stages 2 and 4 only, which is consistent with the lack of sulfate ester formation in Stage 1 (*14*).

4.5 Discussion

4.5.1 Acidity and Particle-Phase Reactions

The observed enhancement in the OC mass concentration with increasing acidity of the inorganic seed aerosol (see Figure 4.1) is consistent with acid-catalyzed particle-phase reactions occurring. These observed enhancements in OC are consistent with prior isoprene studies by Edney et al. (*6*) and Kleindienst et al. (*7*), in which both generated aerosol acidity by the photooxidation of SO_2. The addition of the inorganic seed aerosol in the present study had no significant effect on the gas-phase chemistry (see Table 4.2); therefore, the enhancement of the OC mass is expected to arise only from acid-catalyzed particle-phase reactions.

Further chemical evidence for acid-catalyzed particle-phase reactions was obtained by our organic analysis. The aerosol mass concentrations for the 2-methyltetrols, as well the newly identified sulfate esters (e.g. MW 261 sulfate ester), both of which serve as organic tracers for isoprene SOA in ambient aerosol (*6*, *14*), increased significantly with enhanced aerosol acidity (see Figure 4.4). The exact chemical mechanism for 2-methyltetrol formation remains unclear, as several different pathways may be possible (*11*, *34*). Previous laboratory studies have demonstrated their formation by multiphase acid-catalyzed reactions of isoprene and/or its known oxidation gas-phase products (2-methyl-3-butene-1,2-diol and/or 2-methyl-2-vinyloxirane) with H_2O_2 (*34*, *35*). Alternatively, Wang et al. (*36*) proposed from mass spectral data that 2-methyltetrol formation may also result from acid-catalyzed hydrolysis of epoxydiol intermediates;

however, there is no direct chemical evidence for these intermediates. In addition to 2-methyltetrol and sulfate ester formation, high-MW isoprene SOA products were observed, consistent with prior work (*11*, *23*), and likely result from particle-phase oligomerization reactions.

Despite the observed enhancement of these isoprene SOA products (i.e. 2-methyltetrols, sulfate esters, and high-MW species), it is currently difficult to isolate which reactions dominate the observed acid-effect. Since most laboratory experiments have used sulfuric acid to generate aerosol acidity, using sulfur-free acidic seed aerosol in future isoprene photooxidation experiments could further constrain our understanding of the acid-effect, as sulfate ester formation would not occur. The level of NO_x and its effect on the enhancement of SOA mass when acidic seed is present should also be further investigated, as a prior study by Surratt et al. (*11*) only observed an enhancement in the SOA mass at NO_x-free (low-NO_x) conditions. Dommen et al. (*23*) showed that the volatility of isoprene SOA decreased with decreasing RH; however, acidity generated from inorganic seed aerosol was not employed in that study. The effect of aerosol acidity on SOA formation from isoprene should be further explored at various relative humidities.

4.5.2 Atmospheric Implications

Aerosol acidities have been observed to exceed 300 nmol H^+ m^{-3} during episodes of high photochemical activity throughout several locations of the eastern U.S. (*27*, *29*), which indicates that the range of acidities measured in the present study are atmospherically relevant. For example, Liu et al. (*29*) observed an aerosol acidity of up to 400 nmol H^+ m^{-3} in particles collected from Uniontown, Pennsylvania (a semi-rural site where NH_3 neutralization is incomplete). In addition, Lewandowski et al. (*37*) recently showed that collected ambient $PM_{2.5}$ from the Research Triangle Park, NC area had a greater fraction of 2-methyltetrols and 2-methylglyceric acid contributing to the OC mass when the aerosol was acidic, further demonstrating the atmospheric significance of our findings. In another field study, Kourtchev et al. (*38*) similarly showed that ambient $PM_{2.5}$ aerosol collected at a boreal forest site (Hyytiälä, Finland) also had a greater fraction of 2-methyltetrols during an episode that was characterized by increased SO_2 concentrations, which would likely result in increased aerosol acidity.

The empirical relationship between OC mass and aerosol acidity derived from this study may be useful for regional and global scale atmospheric models, although we caution that the present data were obtained at 30% RH, and it will be necessary to carry out comparable experiments over a range of RH values to evaluate the robustness of the relationship derived here. As was recently shown by Henze and Seinfeld (*22*), including isoprene into a global model significantly increased the overall SOA burden from all sources. Including the impact of acidity on SOA formation from isoprene in such a model, especially in areas where ambient aerosol is known to be acidic, such as the eastern U.S. (*29*), could result in decreasing the gap between modeled predictions of OC aerosol mass concentrations and those actually observed in the atmosphere.

4.6 Acknowledgements

Research at Caltech was funded by the U.S. Environmental Protection Agency Science to Achieve Results (STAR) program grant no. RD-83107501-0, managed by EPA's Office of Research and Development (ORD), National Center for Environmental Research (NCER) and Cooperative Agreement CR-831194001, and by the U.S.

Department of Energy, Biological, and Environmental Research Program DE-FG02-05ER63983. This article has been jointly developed and published by EPA and the California Institute of Technology. It was produced under Cooperative Agreement CR83194001 and is subject to 40 CFR 30.36. The article has been reviewed by EPA personnel under EPA scientific and technical peer review procedures and approved for joint publication based on its scientific merit, technical accuracy, or contribution to advancing public understanding of environmental protection. However, the Agency's decision to publish the article jointly with Caltech is intended to further the public purpose supported by Cooperative Agreement no. CR83194001 and not to establish an official EPA rule, regulation, guidance, or policy through the publication of this article. The U.S. Environmental Protection Agency through its Office of Research and Development also funded research described here under Contract EP-D-05-065 to Alion Science and Technology. Further, EPA does not endorse any products or commercial services mentioned in this publication. J.D.S. was supported in part by the United States Environmental Protection Agency (EPA) under the Science to Achieve Results (STAR) Graduate Fellowship Program.

4.7 Literature Cited

(1) Jang, M.; Czoschke, N. M.; Lee, S.; Kamens, R. M. Heterogeneous atmospheric aerosol production by acid-catalyzed particle-phase reactions. *Science* **2002**, *298*, 814−817.

(2) Iinuma, Y.; Böge, O.; Gnauk, T.; Herrmann, H. Aerosol-chamber study of the α-pinene/O_3 reaction: influence of particle acidity on aerosol yields and products. *Atmos. Environ.* **2004**, *38*, 761−773.

(3) Tolocka, M. P.; Jang, M.; Ginter, J. M.; Cox, F. J.; Kamens, R. M.; Johnston, M. V. Formation of oligomers in secondary organic aerosol. *Environ. Sci. Technol.* **2004**, *38*, 1428−1434.

(4) Gao, S.; Keywood, M.; Ng, N. L.; Surratt, J. D.; Varutbangkul, V.; Bahreini, R.; Flagan, R. C.; Seinfeld, J. H. Low-molecular-weight and oligomeric components in secondary organic aerosol from the ozonolysis of cycloalkenes and α-pinene. *J. Phys. Chem.* **2004**, *108*, 10147−10164; 10.1021/jp047466e.

(5) Gao, S.; Ng, N. L.; Keywood, M.; Varutbangkul, V.; Bahreini, R.; Nenes, A.; He, J.; Yoo, K. Y.; Beauchamp, J. L.; Hodyss, R. P.; Flagan, R. C.; Seinfeld, J. H. Particle phase acidity and oligomer formation in secondary organic aerosol. *Environ. Sci. Technol.* **2004**, *38*, 6582−6589.

(6) Edney, E. O.; Kleindienst T. E.; Jaoui, M.; Lewandowski, M.; Offenberg, J. H.; Wang, W.; Claeys, M. Formation of 2-methyl tetrols and 2-methylglyceric acid in secondary organic aerosol from laboratory irradiated isoprene/NO_x/SO_2/air mixtures and their detection in ambient $PM_{2.5}$ samples collected in the eastern United States. *Atmos. Environ.* **2005**, *39*, 5281−5289.

(7) Kleindienst, T. E.; Edney, E. O.; Lewandowski, M.; Offenberg, J. H.; Jaoui, M. Secondary organic carbon and aerosol yields from the irradiations of isoprene and α-pinene in the presence of NO_x and SO_2. *Environ. Sci. Technol.* **2006**, *40*, 3807−3812.

(8) Tobias, H. J.; Ziemann, P. J. Thermal desorption mass spectrometric analysis of organic aerosol formed from reactions of 1-tetradecene and O_3 in the presence of alcohols and carboxylic acids. *Environ. Sci. Technol.* **2000**, *34*, 2105−2115.

(9) Docherty, K. S.; Wu, W.; Lim, Y. B.; Ziemann, P. J. Contributions of organic peroxides to secondary aerosol formed from reactions of monoterpenes with O_3. *Environ. Sci. Technol.* **2005**, *39*, 4049−4059.

(10) Kalberer, M.; Paulsen, D.; Sax, M.; Steinbacher, M.; Dommen, J.; Prevot, A. S. H.; Fisseha, R.; Weingartner, E.; Frankevich, V.; Zenobi, R.; Baltensperger, U. Identification of polymers as major components of atmospheric organic aerosols. *Science* **2004**, *303*, 1659−1662.

(11) Surratt, J. D.; Murphy, S. M.; Kroll, J. H.; Ng, N. L.; Hildebrandt, L.; Sorooshian, A.; Szmigielski, R.; Vermeylen, R.; Maenhaut, W.; Claeys, M.; Flagan, R. C.; Seinfeld, J. H. Chemical composition of secondary organic aerosol formed from the photooxidation of isoprene. *J. Phys. Chem. A.* **2006**, *110*, 9665−9690.

(12) Barsanti, K. C.; Pankow, J. F. Thermodynamics of the formation of atmospheric organic particulate matter by accretion reactions – part 1: aldehydes and ketones. *Atmos. Environ.* **2004**, *38*, 4371−4282.

(13) Barsanti, K. C.; Pankow, J. F. Thermodynamics of the formation of atmospheric organic particulate matter by accretion reactions – part 2: dialdehydes, methylglyoxal, and diketones. *Atmos. Environ.* **2005**, *39*, 6597−6607.

(14) Surratt, J. D.; Kroll, J. H.; Kleindienst, T. E.; Edney, E. O.; Claeys, M.; Sorooshian, A.; Ng, N. L.; Offenberg, J. H.; Lewandowski, M.; Jaoui, M.; Flagan, R. C.; Seinfeld, J. H. Evidence for organosulfates in secondary organic aerosol. *Environ. Sci. Technol.* **2007**, *41*, 517−527.

(15) Liggio, J.; Li, S. M.; McLaren, R. Heterogeneous reactions of glyoxal on particulate matter: identification of acetals and sulfate esters. Environ. Sci. Technol. 2005, 39, 1532−1541.

(16) Liggio, J.; Li, S. M. Organosulfate formation during the uptake of pinonaldehyde on acidic sulfate aerosols. *Geophys. Res. Lett.* **2006**, *33*, L13808, doi:10.1029/2006GL026079.

(17) Iinuma, Y.; Müller, C.; Böge, O.; Gnauk, T.; Herrmann, H. The formation of organic sulfate esters in the limonene ozonolysis secondary organic aerosol (SOA) under acidic conditions. *Atmos. Environ.* **2007**, doi:10.1016/j.atmosenv.2007.03.007

(18) Limbeck, A.; Kulmala, M.; Puxbaum, H. Secondary organic aerosol formation in the atmosphere via heterogeneous reaction of gaseous isoprene on acidic particles. *Geophys. Res. Lett.* **2003**, *30*, 1996−1999.

(19) Claeys, M.; Graham, B.; Vas, G.; Wang, W.; Vermeylen, R.; Pashynska, V.; Cafmeyer, J.; Guyon, P.; Andreae, M. O.; Artaxo, P.; Maenhaut, W. Formation of secondary organic aerosols through photooxidation of isoprene. *Science* **2004**, *303*, 1173−1176.

(20) Kroll, J. H.; Ng, N. L.; Murphy, S. M.; Flagan, R. C.; Seinfeld, J. H. Secondary organic aerosol formation from isoprene photooxidation under high-NO_x conditions. *Geophys. Res. Lett.* **2005**, *32*, L18808, doi:10.1029/2005GL023637.

(21) Kroll, J. H., Ng, N. L.; Murphy, S. M.; Flagan, R. C.; Seinfeld, J. H. Secondary organic aerosol formation from isoprene photooxidation. *Environ. Sci. Technol.* **2006**, *40*, 1869−1877.

(22) Henze, D. K.; Seinfeld, J. H. Global secondary organic aerosol from isoprene oxidation. *Geophys. Res. Lett.* **2006**, *33*, L09812, doi:10.1029/2006GL025976.

(23) Dommen, J.; Metzger, A.; Duplissy, J.; Kalberer, M.; Alfarra, M. R.; Gascho, A.; Weingartner, E.; Prevot, A. S. H.; Verheggen, B.; Baltensperger, U. Laboratory observation of oligomers in the aerosol from isoprene/NO_x photooxidation. *Geophys. Res. Lett.* **2006**, *33*, L13805, doi:10.1029/2006GL026523.

(24) Birch, M. E.; Cary, R. A. Elemental carbon-based method for monitoring occupational exposures to particulate diesel exhaust. *Aerosol Sci. Technol.* **1996**, *24*, 221−241.

(25) Jaoui, M.; Kleindienst, T. E.; Lewandowski, M.; Edney, E. O. Identification and quantification of aerosol polar oxygenated compounds bearing carboxylic and/or hydroxyl groups. 1. Method Development. *Anal. Chem.* **2004**, *76*, 4765−4778.

(26) Jaoui, M.; Corse, E.; Kleindienst, T. E.; Offenberg, J. H.; Lewandowski, M.; Edney, E. O. Analysis of secondary organic aerosol compounds from the photooxidation of *d*-limonene in the presence of NO_x and their detection in ambient $PM_{2.5}$. *Environ. Sci. Technol.* **2006**, *40*, 3819−3828.

(27) Lioy, P. J.; Samson, P. J.; Tanner, R. L.; Leaderer, B. P.; Minnich, T.; Lyons, W. The distribution and transport of sulfate "species" in the New York metropolitan area during the 1977 summer aerosol study. *Atmos. Environ.* **1980**, *14*, 1391−1407.

(28) Koutrakis, P.; Wolfson, J. M.; Spengler, J. D. An improved method for measuring aerosol strong acidity: results from a nine-month study in St. Louis, Missouri and Kingston, Tennessee. *Atmos. Environ.* **1988**, *22*, 157−162.

(29) Liu, L.-J. S.; Burton, R.; Wilson, W. E.; Koutrakis, P. Comparison of aerosol acidity in urban and semi-rural environments. *Atmos. Environ.* **1996**, *30*, 1237−1245.

(30) Miyoshi, A.; Hatakeyama, S.; Washida, N. OH radical-initiated photooxidation of isoprene: an estimate of global CO production. *J. Geophys. Res.* **1994**, *99*, 18779−18787.

(31) Ruppert, L.; Becker, K. H. A product study of the OH radical-initiated oxidation of isoprene: formation of C_5-unsaturated diols. *Atmos. Environ.* **2000**, *34*, 1529−1542.

(32) Szmigielski, R.; Surratt, J. D.; Vermeylen, R.; Szmigielska, K.; Kroll, J. H.; Ng, N. L.; Murphy, S. M.; Sorooshian, A.; Seinfeld, J. H.; Claeys, M. Characterization of 2-methylglyceric acid oligomers in secondary organic aerosol formed from the photooxidation of isoprene using trimethylsilylation and gas chromatography / ion trap mass spectrometry. *J. Mass. Spectrom.* **2007**, *42*, 101−116.

(33) Kalberer, M.; Sax, M.; Samburova, V. Molecular size evolution of oligomers in organic aerosols collected in urban atmospheres and generated in a smog chamber. *Environ. Sci. Technol.* **2006**, *40*, 5917−5922.

(34) Böge, O.; Miao, Y.; Plewka, A.; Herrmann, H. Formation of secondary organic particle phase compounds from isoprene gas-phase oxidation products: An aerosol chamber and field study. *Atmos. Environ.* **2006**, *40*, 2501−2509.

(35) Claeys, M.; Wang, W.; Ion, A. C.; Kourtchev, I.; Gelencsér, A.; Maenhaut, W. Formation of secondary organic aerosols from isoprene and its gas-phase oxidation products through reaction with hydrogen peroxide. *Atmos. Environ.* **2004**, *38*, 4093−4098.

(36) Wang, W.; Kourtchev, I.; Graham, B.; Cafmeyer, J.; Maenhaut, W.; Claeys, M. Characterization of oxygenated derivatives of isoprene related to 2-methyltetrols in Amazonian aerosols using trimethylsilylation and gas chromatography/ion trap mass spectrometry. *Rapid Commun. Mass Spectrom.* **2005**, *19*, 1343−1351.

(37) Lewandowski, M.; Jaoui, M.; Kleindienst, T. E.; Offenberg, J. H.; Edney, E. O. Composition of $PM_{2.5}$ during the summer of 2003 in Research Triangle Park, North Carolina. *Atmos. Environ.* **2007**, doi:10.1016/j.atmosenv.2007.01.012.

(38) Kourtchev, I.; Ruuskanen, T. M.; Keronen, P.; Sogacheva, L.; Maso, M. D.; Reissell, A.; Chi, X.; Vermeylen, R.; Kulmala, M.; Maenhaut, W.; Claeys, M. Determination of isoprene and a-/b-pinene oxidation products in boreal forest aerosols from Hyytiälä, Finland: Diurnal variations and possible link with particle formation events. *Plant Biology* **2007**, doi: 10.1055/s-2007-964945.

Table 4.1. Input conditions for isoprene/NO four-stage steady-state photooxidation experiment.[a]

parameter	stage 1	stage 2	stage 3	stage 4
isoprene (ppmC)	15.4	15.7	16.0	16.3
NO (ppbv)	300	300	300	300
atomizing solution composition	$(NH_4)_2SO_4$	$(NH_4)_2SO_4$ / H_2SO_4	H_2SO_4	H_2SO_4
atomizing solution concentration (mg L^{-1})	0.5	41 / 60	90	90

[a] 4 hour residence time

Table 4.2. Steady-state concentrations of gas-phase compounds.

compound[a]	stage 1	stage 2	stage 3	stage 4
isoprene (ppmC)	6.6	6.7	6.9	6.8
NO	0.002	0.002	0.002	0.002
NO_x	0.133	0.135	0.134	0.137
O_3	0.149	0.139	0.121	0.122
HNO_3	13	19	26	30
formaldehyde	1070	1000	1110	990
acetaldehyde	39	38	49	48
acrolein	0	14	26	21
acetone	51	58	78	72
methyl vinyl ketone	290	250	320	270
methacrolein	430	390	470	420
glyoxal	58	56	75	77
methylglyoxal	190	180	210	200

[a] Except for isoprene, mixing ratios for all other compounds listed are in ppbv.

Table 4.3. Reacted isoprene and steady-state particle-phase concentrations.

parameter	**stage 1**	**stage 2**	**stage 3**	**stage 4**
reacted isoprene (ppmC)	8.8	9.1	9.0	9.5
organic carbon (μg C m^{-3})	12.2 ± 1.0	20.7 ± 0.1	26.6 ± 3.4	31.1 ± 1.3
[H^+] (nmol H^+ m^{-3})	32	275	407	517
filter mass (μg m^{-3})	17.4	67.4	67.9	104

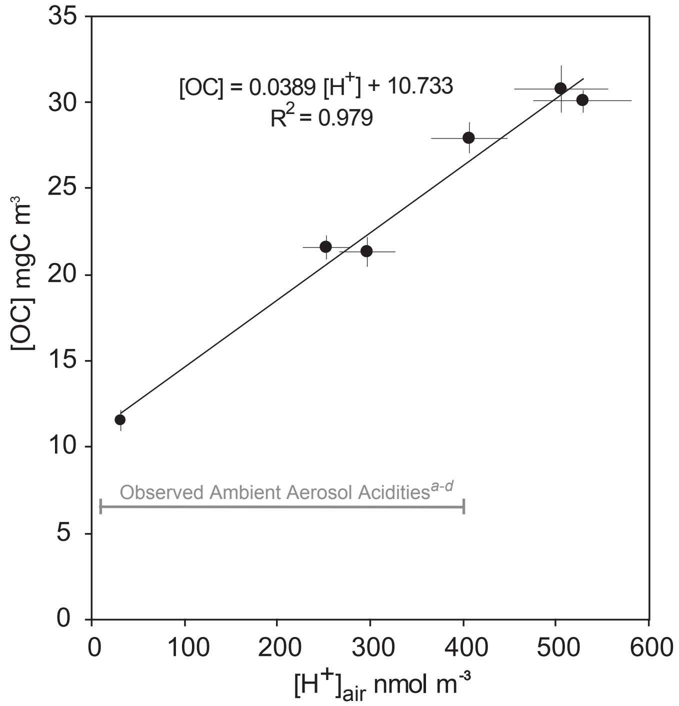

Figure 4.1. Organic carbon concentration as a function of aerosol acidity. The range of ambient $[H^+]_{air}$ shown here include both average and maximum values (episodes of high photochemical activity) observed at several locations in the eastern U.S. [a]Lioy et al. (*27*). [b]Koutrakis et al. (*28*). [c]Liu et al. (*29*). [d]Lewandowski et al. (*37*).

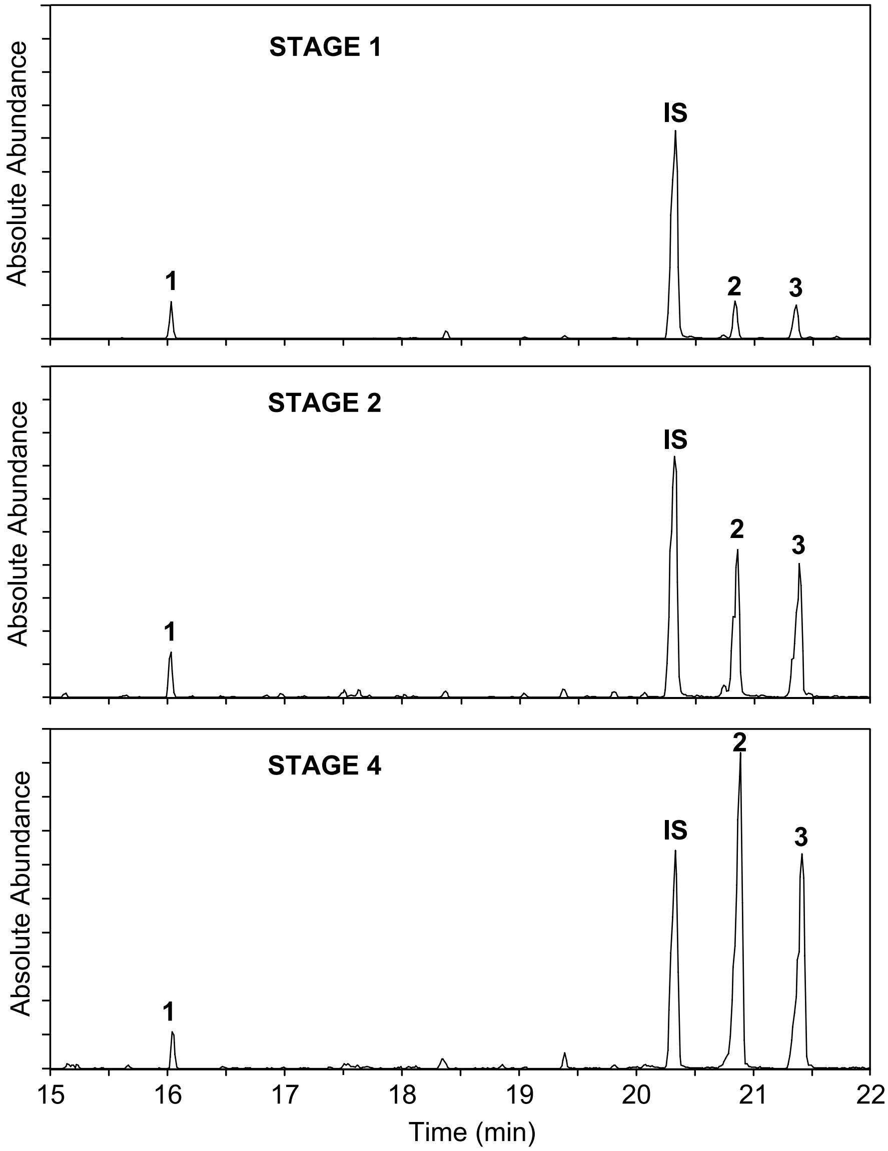

Figure 4.2. Extracted ion chromatograms (*m/z* 165, 321, and 409) for the isoprene / NO photooxidation steady-state experiment. Note that the absolute scales on the three panels are the same. Peak identifications: (1) 2-methylglyceric acid; (IS) *cis*-ketopinic acid internal standard; (2) 2-methylthreitol; and (3) 2-methylerythritol. Internal standard peak areas are within 10% of each other.

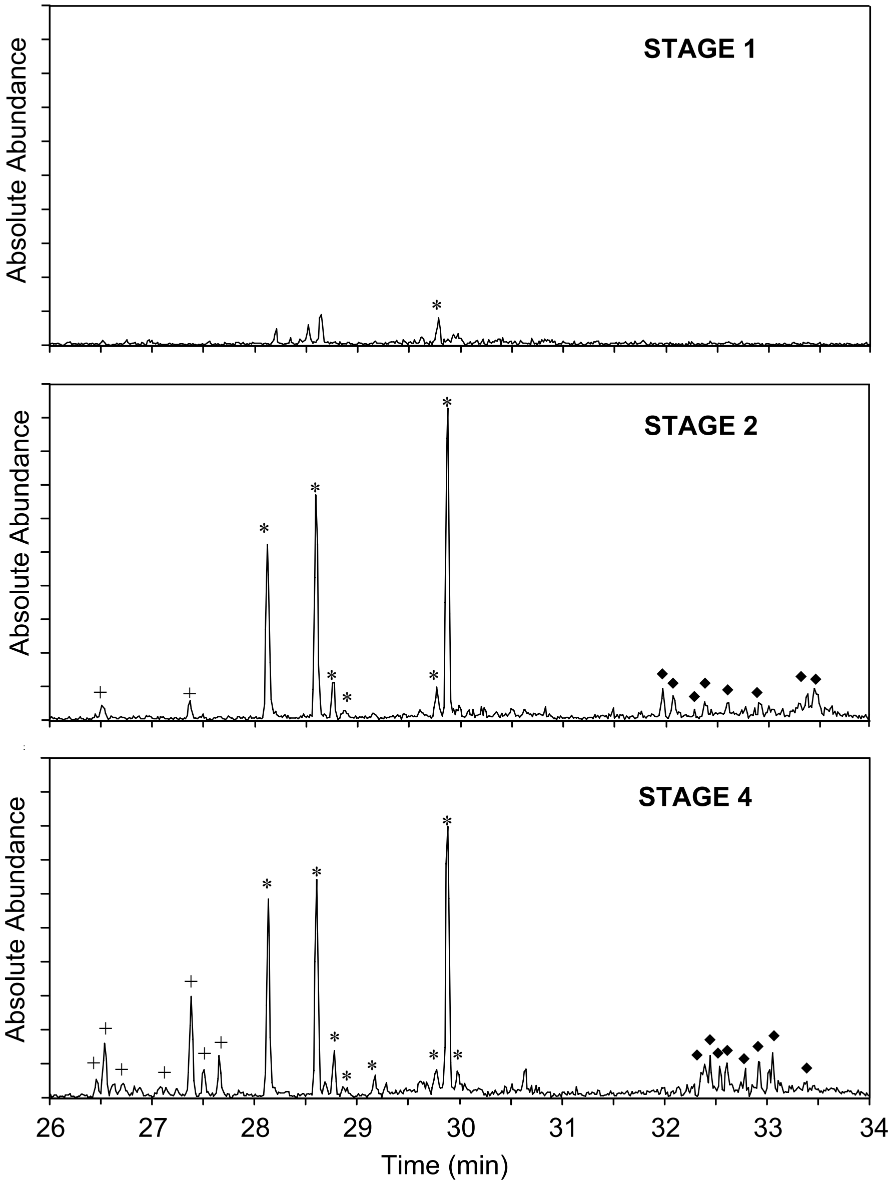

Figure 4.3. Extracted ion chromatograms (*m/z* 407, 495, and 597) for isoprene / NO photooxidation steady-state experiment. Compounds detected as trimethylsilyl derivatives: MW 422 (+); MW 510 (*) (compound tentatively identified by Surratt et al. (*11*) as a 2-methylglyceric acid dimer); MW 612 (◆). Note that the absolute scales on the three panels are the same.

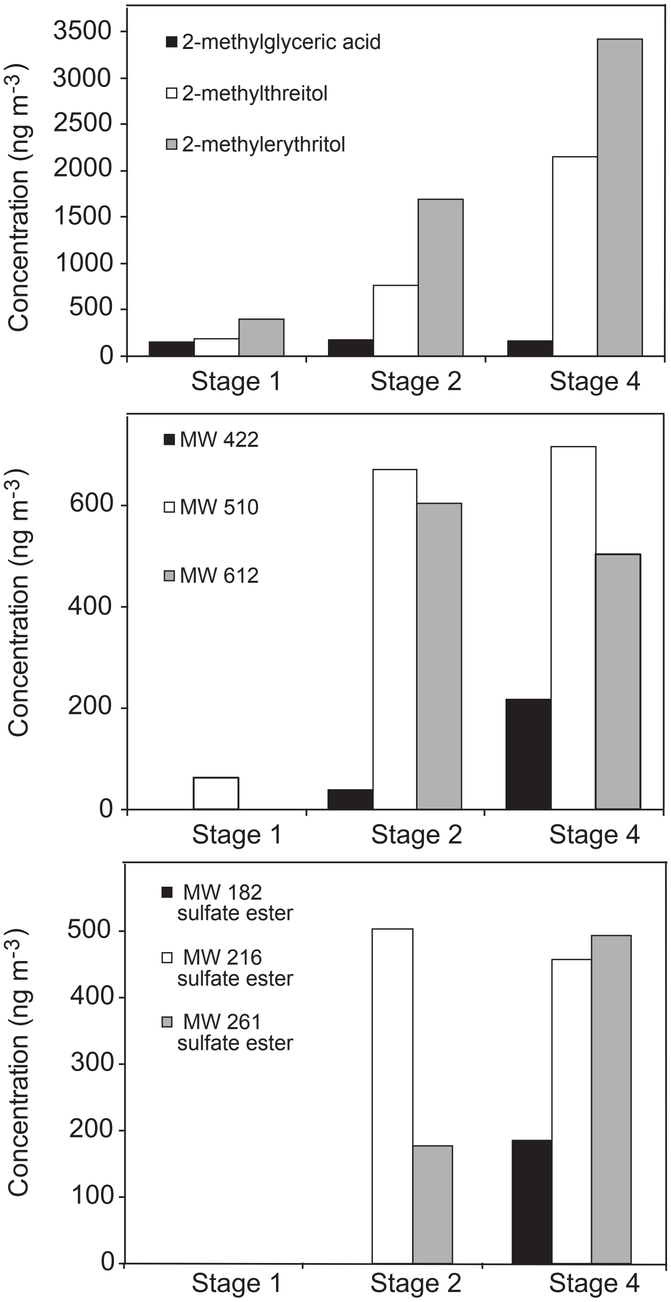

Figure 4.4. Estimated concentrations of several particle-phase SOA products (ng m^{-3})

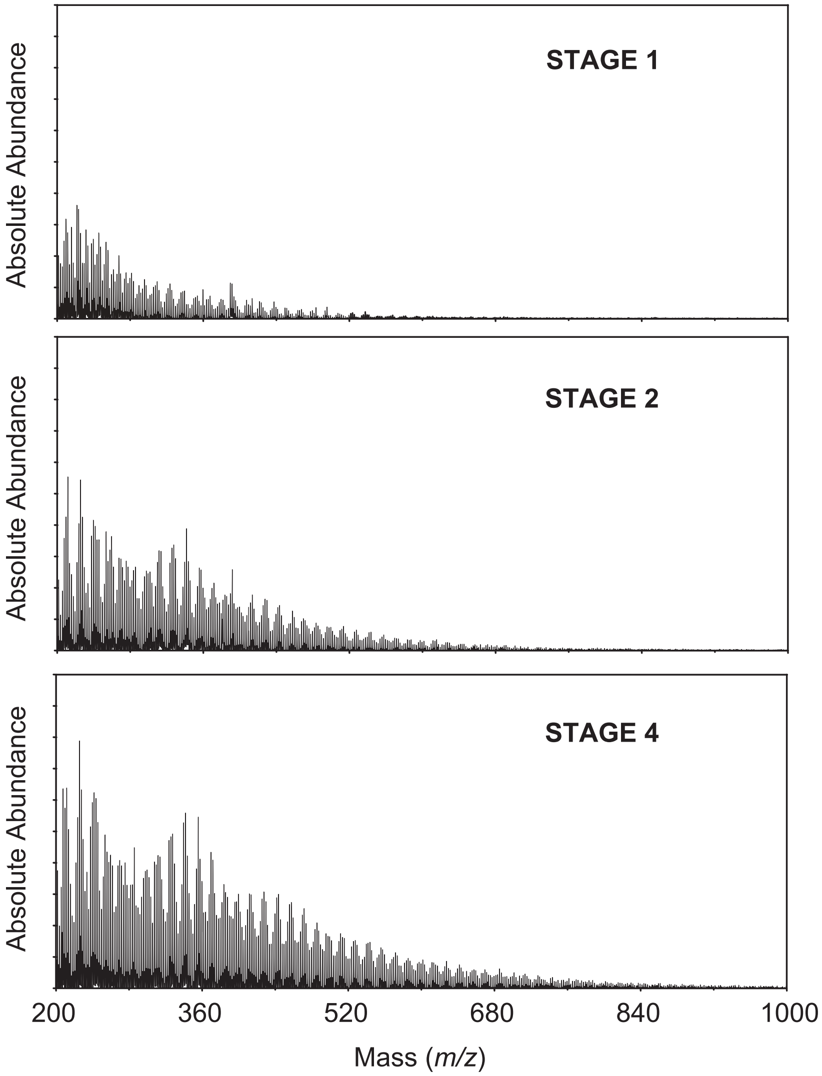

Figure 4.5. (+)MALDI-TOFMS spectra show that increasing particle-phase acidity leads to increased abundances and MWs of isoprene SOA products. Each of the filter samples is based on 20.16 m^3 of sampled chamber air; therefore, owing to the same amount of sample extract applied to the target plate and same amount of chamber air sampled, these spectra are directly comparable. Note that the absolute scales on the three panels are the same.